Research Article Vol. 1, No. 2 / 15 Feb 2022 / Optics Continuum 171

OPTICS CONTINUUM

Measurements and analysis of response function of cold atoms in optical molasses

SUBHAJIT BHAR,[1] MAHESWAR SWAR,[1] URBASHI SATPATHI,[2] SUPURNA SINHA,[1] RAFAEL SORKIN,[3] SAPTARISHI CHAUDHURI,[1] AND SANJUKTA ROY[1,*]

[1]*Raman Research Institute, C. V. Raman Avenue, Sadashivanagar, Bangalore 560080, India*
[2]*International Centre for Theoretical Sciences, Tata Institute of Fundamental Research, Bangalore 560089, India*
[3]*Perimeter Institute for Theoretical Physics, 31 Caroline Street North, Waterloo, ON N2L 2Y5, Canada*
[*]*sanjukta@rri.res.in*

Abstract: We report our experimental measurements and theoretical analysis of the position response function of cold atoms in a magneto-optical trap (MOT) by applying a transient homogeneous magnetic field as a perturbing force. We observe a transition from a damped oscillatory motion to an over-damped relaxation, stemming from a competition between the viscous drag provided by the optical molasses and the restoring force of the MOT. Our observations are in agreement with the predictions of our model based on the Langevin equation. We also study the diffusion of the atomic cloud in the optical molasses and find the measured value of diffusion coefficient matching with the prediction of our theoretical model.

1. Introduction

The response of a physical system to an applied force can reveal intrinsic characteristics of the system such as electric polarisability, impedance of an electronic circuit, magnetic susceptibility and optical conductivity [1–5]. In a similar context, but without the applied force, the study of diffusive behaviour can provide crucial information regarding transport properties [6–8].

In recent years, the diffusion of a Brownian particle in the presence of quantum zero-point fluctuations was analysed in [9,10] starting from the fluctuation-dissipation theorem (FDT) [1,3]. The key input to the analysis presented in [10] is the position response function that describes how the particle reacts to an externally applied force.

The specific response function employed in that paper was suggested by the model of a viscous medium. In the present work, we study a concrete experimental realization of such a model, by utilising a three-dimensional configuration of laser beams known as 'optical molasses' which enables cooling as well as viscous confinement of the atomic cloud. We find agreement (in a classical regime) with the type of response function that was assumed in [10].

Aside from the intrinsic interest of a direct measurement of the response function, our experiment lays the groundwork for future experiments that would access the deep quantum regime, where some of the most interesting effects discussed in [10] would show up.

In this paper, we demonstrate a method to measure the position response function of a cold atomic cloud in a MOT by temporarily subjecting it to a homogeneous magnetic field (transient oscillation method [11]). We observe a transition from a damped oscillatory motion to an over-damped motion of the atomic cloud. This transition stems from a competition between the reactive spring-like force coming from the magneto-optical trap and the viscous drag due to the optical molasses.

In this work, we demonstrate that a simple model based on the Langevin equation can be used to describe the dynamics of the atoms in a MOT in the standard operating conditions at cooling beam intensities larger than the saturation intensity without utilizing approximations such as

#448535 https://doi.org/10.1364/OPTCON.448535
Journal © 2022 Received 18 Nov 2021; revised 22 Dec 2021; accepted 22 Dec 2021; published 24 Jan 2022

OPTICS CONTINUUM

low intensities of the cooling beams used in [11] . Moreover, our model enables us to extract microscopic quantities such as the damping coefficient via measurement of the macroscopic response function.

By turning off the MOT magnetic field, we are also able to study the spatial diffusion of the cold atoms in the viscous medium of an optical molasses, and we verify the Stokes-Einstein-Smoluchowski relation, as described in more detail in Appendix B.

The motion of a Brownian particle can be analysed in terms of either the Fluctuation-Dissipation theorem or the Langevin equation. The FDT (which holds both classically and quantum mechanically) relates the spontaneous position and velocity fluctuations of a system in thermal equilibrium to its linear response to an external perturbing force. This allows the spontaneous fluctuations to be determined from the time-dependent response-function and vice versa.

The Langevin equation [1–3,12–19] (in its classical, generalised, and quantum forms) offers a complementary approach which relates the response function directly to the fluctuating forces that drive the position-fluctuations.

In this paper, we have adopted the Langevin equation as our starting point, since it enables easy identification of all the forces coming into play. In applying it to the theoretical analysis of the dynamics governing the motion of the cold atoms, we have treated the MOT as an interesting example of an out of equilibrium system, and we have studied it from the point of view of statistical physics, rather than from the viewpoint of cold atom experimenters for whom it serves as a valuable and well-documented source of cold atoms. This type of analysis can be extended to a variety of physical situations where one is interested in the motion of particles in a viscous medium.

The paper is organised as follows: In Sec. 2, we briefly describe our experimental setup and methods for preparation and detection of the cold atoms. Sec. 3 is devoted to the position response function of the cold atomic cloud. In Sec. 3.1, we set up the theoretical perspective. In Sec. 3.2, we describe our method for measuring the response function of the cold atoms, and in Sec. 3.3, we compare the analytical results with the experimental observations. In Sec. 4, we present some concluding remarks and future perspectives. There are two appendices. The first supplements our treatment of the response function in the body of the paper. The second presents our results on the spatial diffusion of the cold atoms.

2. Preparation and detection of cold atoms

Our experiment uses a cold atomic cloud of ^{87}Rb atoms trapped in a MOT inside an ultra-high vacuum (UHV) region ($\sim 10^{-11}$ mbar) in a glass cell. A schematic diagram of the experimental setup is shown in Fig. 1. The MOT is vapour-loaded from a Rb getter source. An external cavity diode laser (ECDL) serves as the cooling laser, the laser beam being 12 MHz red-detuned from the $5S_{1/2}, F = 2 \rightarrow 5P_{3/2}, F' = 3$ (D_2) transition of ^{87}Rb. Another ECDL, the repump laser, is tuned to the transition, $5S_{1/2}, F = 1 \rightarrow 5P_{3/2}, F' = 2$, and used to optically pump the atoms back into the cooling cycle. This is a standard procedure in laser cooling experiments. The detuning and intensity of the cooling and repump beams are controlled by acousto-optic modulators (AOM). The restoring force required to confine the cold atoms is provided by a pair of current carrying coils in a near ideal anti-Helmholtz configuration.

The fiber coupled laser beams are expanded to have a Gaussian waist diameter of 10 mm and combined in a non-polarizing cube beam splitter. Thereafter, the combined cooling and repump beams are split into three pairs of beams using a combination of half-wave plates and polarizing cube beam splitters. Each of the cooling beams is sent through the UHV glass cell and retro-reflected via a quarter waveplate and a mirror. The incoming cooling beams are kept slightly converging so as to account for the losses in the optical elements and to ensure that any radiation-pressure imbalance between the incoming and the retro-reflected beam is eliminated.

OPTICS CONTINUUM

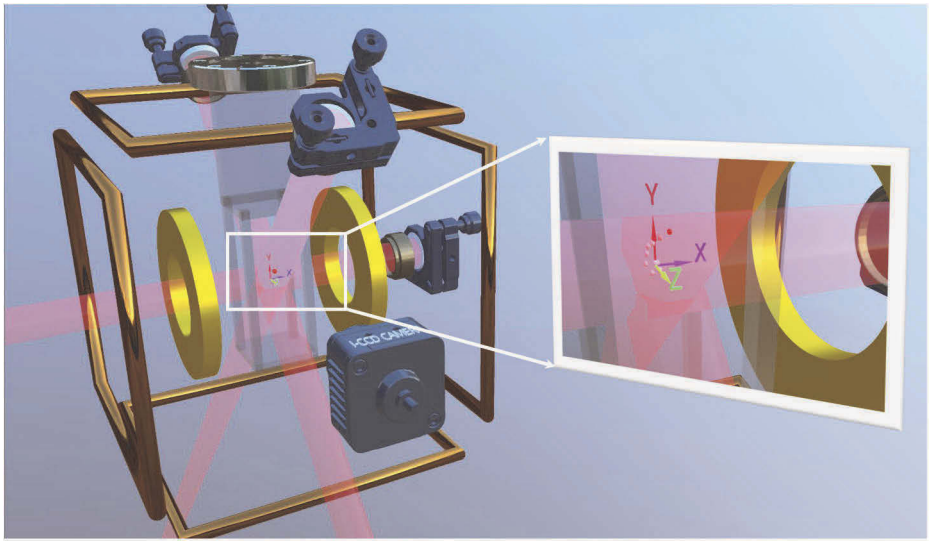

Fig. 1. Schematic diagram of the experimental setup where a cold atomic cloud is produced in a MOT in a glass cell. A magnified view near the cold atomic cloud is shown in the inset. The trajectory of the cold atomic cloud is shown as a series of atomic clouds at successive positions in the XY plane. The cooling beams are retro-reflected using a mirror and a quarter-wave plate. The cylindrical magnetic coils produce the quadrupole magnetic field used for the MOT, and the square coils produce the homogeneous magnetic field used in measuring the response function. The detection of the atomic cloud is done by means of absorption imaging using an ICCD camera.

The cold atoms are detected by a time-of-flight absorption imaging technique, using a short ($\sim 100\ \mu$sec) pulse of weak, resonant linearly polarised laser light tuned to the $5S_{1/2}, F = 2 \rightarrow 5P_{3/2}, F' = 3$ transition. The shadow cast by the atoms is imaged onto an ICCD camera with a magnification factor of 0.4. In a typical run of the experiment, we trap and cool about 5×10^7 atoms at a temperature of around 150 μK.

3. Response function of the cold atoms

3.1. Langevin Equation

Our starting point is the Langevin Equation [20]. In its fully quantum mechanical form, it reads

$$M\ddot{x} + \int_{-\infty}^{t} dt' \alpha(t - t')\dot{x}(t') + kx = \zeta(t) + f(t) \tag{1}$$

where M is the mass of the particle, $\alpha(t)$ is the dissipation kernel, and $\zeta(t)$ is the noise related to the dissipation-kernel via the Fluctuation Dissipation Theorem (FDT) [12] as follows:

$$\begin{aligned} \langle \zeta(t) \rangle &= 0 \\ \langle \{\zeta(t), \zeta(t')\} \rangle &= \frac{2}{\pi} \int_0^\infty d\omega\, \hbar\omega \coth\left(\frac{\hbar\omega}{2k_B T}\right) \\ &\quad \mathrm{Re}[\tilde{\alpha}(\omega)] \cos(\omega(t - t')) \end{aligned} \tag{2}$$

The position-operator, $x(t)$, of the particle at any time t can be obtained by solving these equations.

OPTICS CONTINUUM

The experiments reported here are at high enough temperatures that the noise can be treated classically. We can therefore take the $\hbar \to 0$ limit of the previous equation, to obtain the noise correlators in their classical form:

$$\begin{aligned} \langle \zeta(t) \rangle &= 0 \\ \langle \zeta(t)\zeta(t') \rangle &= \frac{2k_B T}{\pi} \int_0^\infty d\omega \, \mathrm{Re}[\tilde{\alpha}(\omega)] \cos(\omega(t-t')) \end{aligned} \tag{3}$$

(This form of Langevin equation is sometimes termed "generalized" to indicate that the dissipation-kernel is not restricted to being a delta-function.)

The last term on the left-hand side of Eq. (1) corresponds to a harmonic force characterized by a spring constant k. In our present problem kx corresponds to the restoring force of the MOT. The term $f(t)$ on the right-hand side is a perturbing force, which in this experiment is an additional magneto-optical force induced by the transient homogeneous magnetic field used to measure the position-response function.

Taking the expectation value of Eq. (1), and substituting $\langle \zeta(t) \rangle = 0$, we obtain a deterministic equation for $\langle x(t) \rangle$, whose Fourier transform is

$$-M\omega^2 \tilde{x}(\omega) - i\omega\tilde{\alpha}(\omega)\tilde{x}(\omega) + k\tilde{x}(\omega) = \tilde{f}(\omega) \tag{4}$$

(here we have used x to denote the mean position of the particle.) Eq. (4) can be re-expressed as

$$\tilde{x}(\omega) = \tilde{R}(\omega)\tilde{f}(\omega) \, , \tag{5}$$

where

$$\tilde{R}(\omega) = \frac{1}{[-M\omega^2 - i\omega\alpha + k]} \tag{6}$$

is the position response function of the particle (in this case the cold atomic cloud) in the frequency domain.

Here we have set $\tilde{\alpha}(\omega) = \alpha$, corresponding to the choice of an Ohmic bath to which the system is coupled. This choice is motivated by the optical molasses in the cold-atom experimental setup. In fact, an Ohmic bath is equivalent to a force proportional to the velocity with a fixed coefficient of proportionality or damping coefficient. The present experiment serves as a test of this theoretical model of the molasses.

The position response function in the time domain is given by:

$$R(t) = \frac{1}{2\pi} \int \tilde{R}(\omega) e^{-i\omega t} d\omega. \tag{7}$$

The position response function obtained thereby from Eq. (6) for the Ohmic bath is

$$R(t) = \frac{2}{\alpha_c} e^{-\frac{\alpha t}{2M}} \sinh\left(\frac{\alpha_c t}{2M}\right) \tag{8}$$

where $\alpha_c = \sqrt{\alpha^2 - 4kM}$..

There are three qualitatively distinct cases. For $\alpha^2 > 4kM$, α_c is real and one gets an overdamped motion of the cold atomic cloud. For $\alpha^2 = 4kM$, the motion of the cold atomic cloud is critically damped, while for $\alpha^2 < 4kM$, α_c is imaginary and the motion of the cold atomic cloud is a damped oscillation. For $k = 0$, Eq. (8) reduces to the position response function used in [10]. (Note that in the MOT, k is always non-zero due to the presence of the non-zero magnetic field gradient.)

In Sec 3.3, we will compare the analytically calculated motion of the cold atomic cloud that follows from $R(t)$ via Eq. (10) below with the experimentally observed oscillatory and damped motions of the cloud.

OPTICS CONTINUUM

By taking a time derivative of $R(t)$, one can also get the velocity response function,

$$\dot{R}(t) = \frac{1}{\alpha_c M} e^{-\frac{\alpha t}{2M}} \left(\alpha_c \cosh\left(\frac{\alpha_c t}{2M}\right) - \alpha \sinh\left(\frac{\alpha_c t}{2M}\right)\right). \tag{9}$$

It's an interesting fact that the position response function $R(t)$ can be inferred directly from the mean velocity induced by a homogeneous force whose time-dependence is that of a step-function. By definition, the mean displacement $\langle x(t)\rangle$ is related to $R(t)$ by the equation,

$$\langle x(t)\rangle = \int_{-\infty}^{t} R(t-t')f(t')dt' \tag{10}$$

("linear response theory" [9,10]).

On differentiation, this gives the expectation value $\langle v(t)\rangle$ of the velocity:

$$\langle v(t)\rangle = \int_{-\infty}^{t} \dot{R}(t-t')f(t')dt'. \tag{11}$$

Here $f(t)$ is the external perturbing force, which in our experiment takes the form of a "top-hat function", $f(t) = f_0\,\theta(t+w)\,\theta(-t)$:

$$f(t) = \begin{cases} f_0, & \text{for } -w<t<0 \\ 0, & \text{for } t \le -w,\ t \ge 0 \end{cases}. \tag{12}$$

(In our experiment $f(t)$ is induced by a bias field. The temporal profile of this field, together with an analysis of how $f(t)$ depends on it, is given in detail in Appendix A.1.)

Substituting into Eq. (11), we get:

$$\langle v(t)\rangle = f_0 \int_{-w}^{0} \dot{R}(t-t')dt' \tag{13}$$

$$= -f_0\,(R(t) - R(t+w)) \tag{14}$$

$$R(t) = -\frac{1}{f_0}\langle v(t)\rangle + R(t+w). \tag{15}$$

For $w \to \infty$, $R(t+w) \to R(\infty) = 0$. (This assumes that the MOT is turned on. When it is turned off and only the molasses is present, $R(\infty)$ will be non-zero.) Therefore we get

$$R(t) = -\frac{1}{f_0}\langle v(t)\rangle. \tag{16}$$

This simple relationship means that one can measure the position response function directly, simply by measuring the expectation value of the velocity.

3.2. Measurement of the position response function

The theoretical expression (8) for the position response function of the cold atoms contains two unknown parameters, the damping-coefficient α and the spring constant k. In order to test the theoretical model that leads to (8), and at the same time determine the values of the parameters α and k, one needs to observe how the cloud of cold atoms moves in response to an external force.

In our experiment we apply a homogeneous magnetic field (bias field), and then follow the motion of the cloud of cold atoms after the field is switched off. We first prepare the laser-cooled ^{87}Rb atoms in a MOT as described in Sec 2. After that, we apply a homogeneous bias field, B_b. This shifts the trap center to the zero of the new magnetic field. The cold atoms experience a

OPTICS CONTINUUM

force towards the new center, and equilibrate there within a short interval of time. After 5 sec, we turn the bias field off, and the cold atoms return to the initial trap center, following a trajectory from which the position response function can be inferred. To trace the trajectory, we record the position of the cold atoms at regular intervals of time after turning off the bias field.

Fig. 2 is a schematic diagram of the sequence of events in the experiment. We capture and cool the atoms in the MOT from a Rb getter source with a loading time of 15 sec. The cooling beams, having a Gaussian cross-section with a waist size of 10 mm, are red-detuned by 2.2 Γ from the $5S_{1/2}, F = 2 \rightarrow 5P_{3/2}, F' = 3$ transition, where $\Gamma = 38.11(6) \times 10^6 s^{-1}$ ($2\pi \times 6.065(9)$ MHz) is the decay rate (natural line-width) of the ^{87}Rb D_2 transition. Different values of the MOT magnetic field gradient were used in different sets of measurements. For the oscillatory motion shown in Fig. 3, the gradient was 18 Gauss/cm; for the over-damped motion shown in Fig. 4, it was 3.5 Gauss/cm.

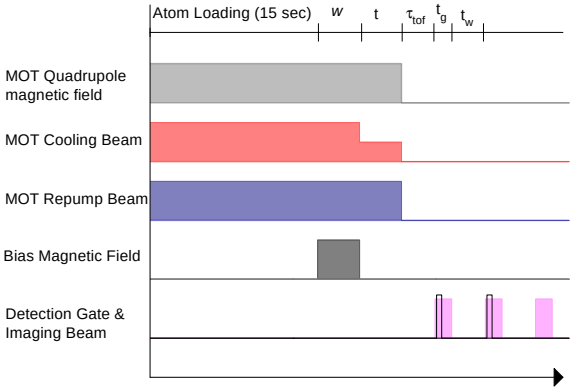

Fig. 2. Timing sequence for measuring the response function of the cold ^{87}Rb atoms. We prepare the cold atomic cloud by loading the MOT for 15 sec. Thereafter, we apply a homogeneous bias magnetic field for 5 sec (w). After the bias field is switched off, the cooling beam detuning and intensity are changed by a variable amount in order to explore a range of values of α. The ensuing motion of the cloud is monitored via time-of-flight absorption imaging. In our experiment, time-of-flight(τ_{tof}) is 1.2 ms, the detection gate time (t_g) is 1 ms, and the pulse width of the imaging beam is 100 μs. The time separation between successive absorption images (t_w) is 1 sec.

After the preparation stage, we apply the bias field for 5 seconds (its amplitude being 3 Gauss for Fig. 3 and 0.6 Gauss for Fig. 4). Thereafter, we turn the bias field off and wait for a variable time t, after which we switch off the quadrupole magnetic field and the cooling and repumper laser beams simultaneously, and take an absorption image after allowing the cloud to move ballistically for a time $\tau_{tof} = 1.2$ ms. The mean position of the cold atomic cloud is inferred by fitting a Gaussian to the column-density profile of the cloud.

3.3. Experimental results and comparisons with the theory

3.3.1. Motion of the cold atoms

In our experimental runs, we allow the cloud to move ballistically for a time $\tau_{tof} = 1.2$ ms after switching off the MOT light beams and the quadrupole field (the bias field having been switched off earlier, of course). This delay lets us acquire the absorption image of the cloud in a magnetic field-free environment.

OPTICS CONTINUUM

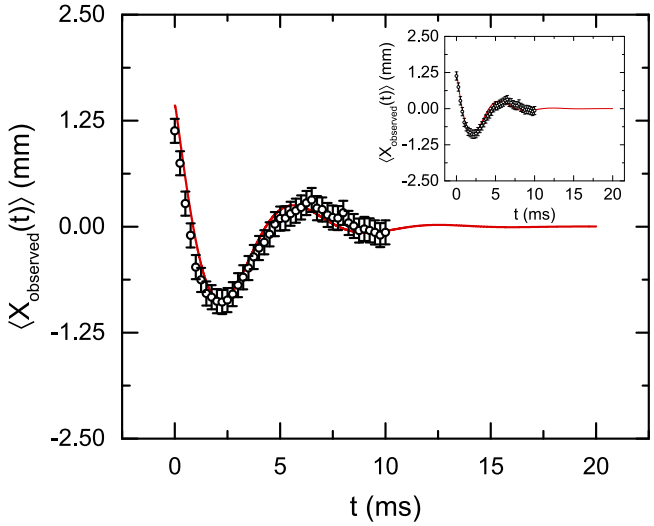

Fig. 3. Position of the cold atoms as a function of time after the homogeneous bias field is switched off, illustrating the underdamped regime. Cooling beam detuning: $-2.2\,\Gamma$, total intensity: $I = 16.91\,I_{sat}$; MOT Magnetic field gradient: 18 G/cm; bias magnetic field: 3 Gauss with its direction at an angle to the image plane. The solid line is the best fit between the experimental data and the theoretical prediction from Eq. (26) with $\alpha = (1.04 \pm 0.04) \times 10^{-22}$ kg/sec. Inset: A test fit of the data to Eq. (18) yielded an initial estimate of $\alpha = (1.06 \pm 0.24) \times 10^{-22}$ kg/sec.

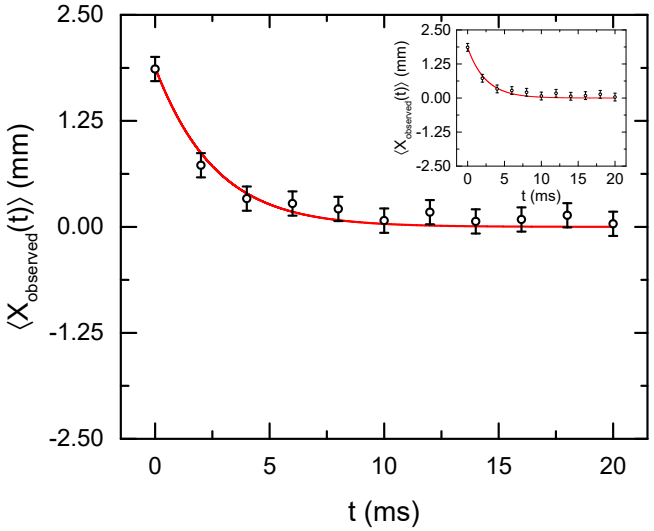

Fig. 4. Position of the cold atoms as a function of time after the homogeneous bias field is switched off, illustrating the overdamped regime. Detuning: $-2.2\,\Gamma$, total intensity I: $9.73\,I_{sat}$; MOT Magnetic field gradient: 3.5 G/cm; bias magnetic field: 0.6 Gauss with its direction along one of the Cartesian axes in the image plane. The solid line exhibits the best fit between the data and Eq. (26) with $\alpha = (1.57 \pm 0.46) \times 10^{-22}$ kg/sec. Inset: A test fit to Eq. (18) yielded an initial estimate of $\alpha = (1.58 \pm 0.24) \times 10^{-22}$ kg/sec.

OPTICS CONTINUUM

However, it introduces a small correction to the mean position of the cloud given by

$$\langle x_{observed} \rangle = \langle x(t) \rangle + \tau_{tof} \langle v(t) \rangle. \tag{17}$$

The graphs in Fig. 3 and Fig. 4 show the time variation of $\langle x_{observed} \rangle$ after the bias field is turned off. Each data point shown is the average of three experimental runs, and the error bar is the standard deviation of the mean position, measured as described in Sec. 3.2.

In Fig. 3, we observe an underdamped oscillatory motion of the cold atomic cloud where the MOT magnetic field gradient is 18 Gauss/cm and the magnitude of the bias field is 3 Gauss along the x-direction as shown in Fig. 1. In Fig. 4, we observe an over-damped motion of the cold atomic cloud where the MOT magnetic field gradient is 3.5 Gauss/cm and the magnitude of the bias field is 0.6 Gauss along the x-direction.

The theoretical curves shown in Fig. 3 and Fig. 4, were obtained by fitting the experimental data to the prediction Eq. (26) (with due regard to Eq. (17)). In these fits, there is only a single fitting parameter: the damping coefficient α.

In the insets to Fig. 3 and Fig. 4, we have fitted the experimental data to the solution of a damped-harmonic oscillator,

$$\langle x(t) \rangle = A\, e^{\frac{(-\alpha+\alpha_c)t}{2M}} + B\, e^{\frac{-(\alpha+\alpha_c)t}{2M}} \tag{18}$$

without assuming anything further about the form of the position response function.

Here α_c is defined as earlier, and $M = 1.44316060(11) \times 10^{-25}$ kg is the mass of the ^{87}Rb atom. The fitting parameters in this case were A, B, and α. From these fits, we obtained our initial estimates of α.

By definition, both the models described by Eq. (26) and Eq. (18) agree that the motion of the cloud after the perturbing force is switched off is that of a damped harmonic oscillator. However, the simpler model based only on this fact yields no information on the Response Function, which is the central concern of our paper. In Fig. 3, the statistical errors associated with the two models (corresponding to Eq. (26) and Eq. (18), respectively) have been mentioned explicitly. They show that the fuller, more predictive treatment which incorporates the form of the perturbing force produces a better fit in the underdamped regime. (In the overdamped regime of Fig. 4, the two models cannot be distinguished by our data.)

An approach based on a similar 3-parameter fit to the motion of an atom in a MOT was presented in [11]. However, while being a correct approximation, it does not capture the details of the external perturbing force in their entirety. In contrast, our approach based on the response function can be used for any form of the perturbing force. Hence it offers a theoretical model which is versatile and widely applicable for this class of experiments.

The experiments reported in [11] are performed in a totally different parameter regime compared to parameter regimes of standard steady-state magneto-optical traps including the ones reported in our manuscript. For example, the authors in [11] have used low cooling beam intensities in the range of 0.1-0.6 mW/cm^2. On the other hand, we have investigated the dynamics of the atoms in a MOT with cooling beam intensities in the range 20 mW/cm^2, which is typically the intensities used for MOTs as a starting point of cold atom experiments.

As discussed in Sec. 3.1, the cold atomic cloud shows an underdamped oscillatory motion or an over-damped motion in response to the applied bias field depending on whether $\alpha^2 < 4kM$ or $\alpha^2 > 4kM$ respectively, i.e. whether the restoring force due to the magneto-optical trapping overwhelms the viscous force due to the optical molasses or vice versa. As always, α here denotes the damping coefficient and k the spring constant corresponding to the MOT. Both α and

OPTICS CONTINUUM

k can be calculated from 1D Doppler cooling theory [21,22] as,

$$\alpha = 4\hbar\kappa^2 s_0 \frac{2|\delta|/\Gamma}{\left(1 + 2s_0 + \frac{4\delta^2}{\Gamma^2}\right)^2} \tag{19}$$

$$k = g\frac{\mu_B \lambda}{h}\alpha \frac{\partial B_m}{\partial x} \tag{20}$$

where λ is the wavelength and $\kappa = 2\pi/\lambda$ is the wavenumber of the cooling beams, δ is the detuning of the cooling beams from the atomic transition, μ_B is the Bohr magneton, $\frac{\partial B_m}{\partial x}$ is the MOT magnetic field gradient and s_0 is the saturation parameter of the cooling beams defined as I/I_{sat} where I is the total intensity of the cooling beams and I_{sat} is the saturation intensity ($I_{sat} = 1.6\,mW/cm^2$ for ^{87}Rb $5S_{1/2}, F = 2 \rightarrow 5P_{3/2}, F' = 3$ transition and $\sigma^{\pm}$ polarised light). Hence, the damping coefficient α depends on the detuning and intensity of the cooling beams of the MOT, while the spring constant k has an additional dependence on the magnetic field gradient.

Using the simplest possible assumption that the fluorescence from the trapped atoms accurately gives the damping co-efficient in our fitting algorithm described above, we obtain a normalised mean square residual of 8.2% and 5% for the data presented in Fig. 3 and Fig. 4 respectively. However, in the presence of a gradient magnetic field in the MOT and for a Gaussian atom number spatial distribution in the atomic cloud and a Gaussian spatial intensity profile of the cooling laser beams, this simple assumption is likely to be inaccurate. Therefore, we kept α to be a free fitting parameter and obtained a normalised mean square residual to be 2.1% and 2.6% for the data presented in Fig. 3 and Fig. 4 respectively. This indicates that while the fluorescence measurements can give a reasonable estimate of the damping coefficient of cold atoms in the MOT, more accurate values of the damping coefficient can be found using experimental measurements which is modelled well using our theoretical description presented in this paper.

3.3.2. Estimation of the damping coefficient (α) in the MOT

In Fig. 5, the damping coefficients (α) obtained from fitting the experimental data with the analytical expression given in Eq. (26) and Eq. (30) are plotted against the light shifts, where the light shift (Δ) is given by:

$$\Delta = \hbar\,|\delta|\,\frac{I/I_{sat}}{1 + 4\delta^2/\Gamma^2} \tag{21}$$

where δ is the detuning of the cooling beam from the atomic transition and Γ is the natural linewidth of the atomic transition having transition wavelength $\simeq$ 780 nm. The data in Fig. 5 shows that the variation of the damping coefficient α with light shift in the MOT is rather slow even though the MOT is operated in a wide range of intensity and detuning. Hence, it is possible to present a consistent treatment of damping over a wide range of parameters following the Langevin equations.

3.3.3. Position response function from velocity

In Fig. 6(a) and Fig. 6(b), we show comparisons between the theoretically obtained position response functions given in Eq. (8) (solid lines) and the experimentally obtained scaled velocities $-\frac{1}{f_0}\langle v(t)\rangle$ (circle with error bars) for the motion of the atomic clouds given in Fig. 3 (oscillatory motion) and Fig. 4 (damped motion). Note that the scaled velocity data agrees very well with the curves for the response functions, confirming Eq. (16), which is indeed a very good approximation to the exact response function (in other words, the top hat function approximates the exact bias field and in turn the perturbing force well).

OPTICS CONTINUUM

As we vary the molasses parameters and the MOT's magnetic field gradient in the experiment, we observe both oscillatory and monotonic motions of the cloud's centroid $\langle x(t)\rangle$, indicating a transition from an underdamped to an over-damped regime. We did not attempt to explore all the parameters (intensity, detuning, magnetic field gradient) in sufficient detail to pin down the exact transition point between the two regimes. Nevertheless, in the reasonably large parameter space that we have explored, the two regimes appear clearly, as does more generally the systematic variation of the response function with the experimental parameters of the MOT.

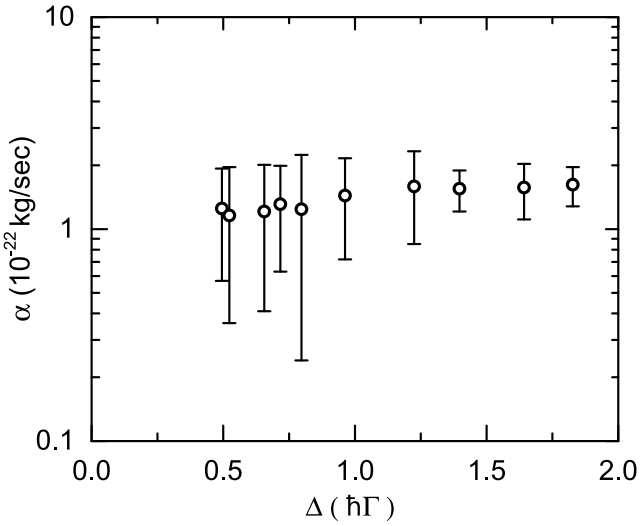

Fig. 5. Damping coefficient (α) as a function of the light shift. MOT magnetic field gradient: 3.5 G/cm. The data was taken in the overdamped regime exemplified by Fig. 4.

OPTICS CONTINUUM

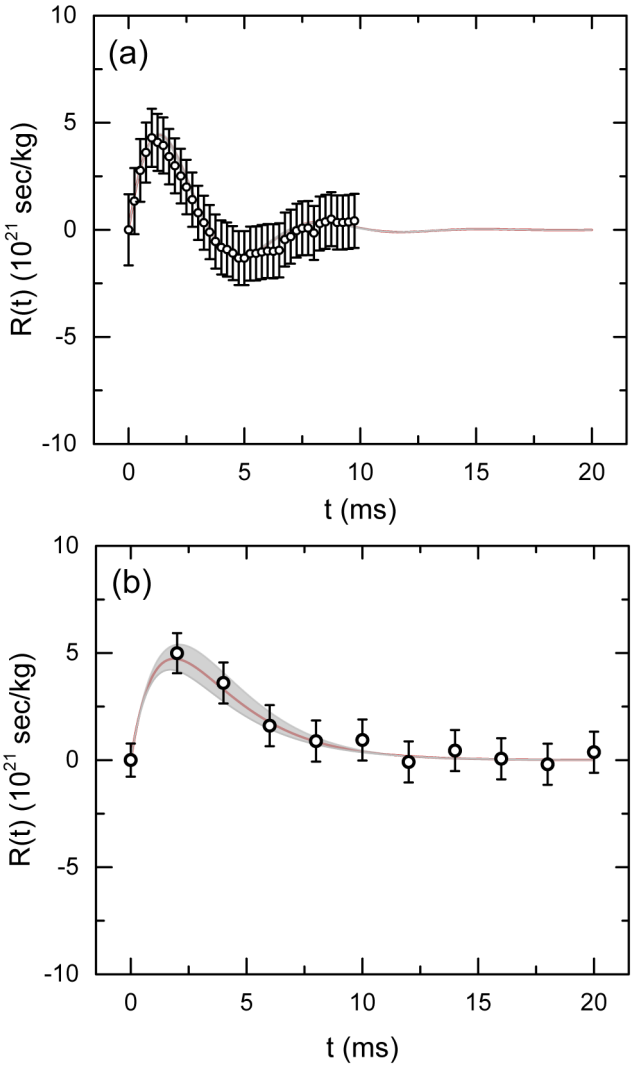

Fig. 6. Position response function deduced directly from velocity for (a) oscillatory motion with $\alpha = (1.04 \pm 0.04) \times 10^{-22}$ kg/sec and (b) damped motion with $\alpha = (1.57 \pm 0.46) \times 10^{-22}$ kg/sec. In both the graphs, solid lines represent the theoretical prediction of $R(t)$ given in Eq. (8) and the shaded region shows the 68% confidence band. The experimental data points correspond to the scaled velocities $-\frac{1}{f_0}\langle v(t)\rangle$ of the cold atoms.

OPTICS CONTINUUM

4. Conclusion and outlook

In this work, we have measured the position response function of the cold atoms in a MOT by subjecting them to a transient homogeneous magnetic field. We have tested theoretical predictions regarding the nature of the response function, and we have done extensive theoretical analysis and numerical modelling of our experimental observations.

One of the significant outcomes of the study has been the verification of the functional form of the position response function which was used as input to a recent theoretical study [10] of diffusion, not only in the classical domain dominated by thermal fluctuations, but also in the still-to-be-explored quantum domain where zero-point fluctuations are the main driver of the diffusion [23].

Our study has led to the experimental observation of a transition from an oscillatory to an over-damped behaviour of the response function as a result of a competition between elastic and dissipative effects. We find a good agreement between our experimental measurements and the theoretical model of a particle moving in a viscous medium and confined by a harmonic-oscillator potential. These measurements can be readily extended to lighter atomic species compared to Rb such as Na and K so as to access a larger range of parameter space to observe a smooth transition of the response function from an under-damped to an over-damped behaviour.

Our results demonstrate that a simple model (based on the Langevin equation) can describe the dynamics of the atoms in a MOT without resorting to further approximations such as low intensity regime in the Doppler theory, where the cooling light intensities are assumed to be small. In the case of optimized operations in a MOT, the cooling light intensities are typically well above the saturation intensity, and our model handles this regime successfully. In contrast, many previous studies (including reference [11]) have considered only low intensity limit, and consequently conducted their experiments in conditions of low-intensity cooling light.

In this work, our model allows us to extract microscopic quantities such as scattering rate from measurements of the macroscopic response function. The knowledge extracted through this study can be applied to multispecies traps, while additional damping due to inter-species light-assisted collision-induced processes can be modelled in the near future. Such studies are significant, because experiments with cold atom mixtures are currently a focus of many research groups, and trap parameter optimizations beyond the low intensity Doppler regime are of interest. Our generalized theoretical description is capable of handling this particular problem.

We also studied the spatial diffusion of the cold atoms in the optical molasses (Appendix B.), observing a behaviour which is consistent with a theoretical model based on the Langevin equation. In particular, the measured value of the diffusion coefficient agreed with the value predicted by the Langevin model, using the damping coefficient deduced from our measurements of the position response function at the same temperature.

One novelty of our theoretical analysis is the observation that the position response function can be obtained directly from the velocity (Eq. (16)) if the temporal variation of the perturbing force is a step function. This is confirmed by our experiment.

Our theoretical analysis also points out that in the MOT where the magnetic field is linearly proportional to the distance from the centre, the magneto-optical force can be written as the gradient of the square of the local magnitude of the magnetic field as shown in Eq. (23) of the first Appendix. This relationship simplified the theoretical modelling of the perturbing force in our experiment as seen in Eq. (24).

We would like to emphasise that the present work is a prelude to the study of diffusion driven by zero-point quantum fluctuations. We have a theoretical prediction for the mean square displacement in this domain, which can be verified in ultracold atom experiments for which the knowledge of the position response function will be crucial. In the present experiment, we have developed a technique to determine the response function empirically, and we have verified, in the present regime, the form we had assumed in making the prediction.

OPTICS CONTINUUM

Our study provides a general framework to analyse the motion of a particle in optical molasses combined with a restoring force, such as in a MOT, ion-traps in the presence of cooling laser beams [24], or ultra-cold atoms in optical lattices in the presence of additional optical molasses [25,26]. These and other similar experimental systems are of current interest in the context of quantum technology devices [27]. This study paves the way for exploring spatial diffusion of ultra-cold atoms in the quantum regime where zero-point fluctuations dominate over thermal ones [9,10,28].

The central questions addressed in this paper are rooted in non-equilibrium statistical mechanics, and the fact that we address them using the tools of cold atom physics, makes this study inherently interdisciplinary in nature. In future, we intend to experimentally measure and analyse the zero-point fluctuation driven diffusion in the quantum domain that has been predicted in [9,10]. In that context, we will expand our perspective beyond the classical Langevin Equation to a fully quantum-mechanical formulation (quantum Langevin equation).

Appendix

A. Theoretical Modelling: Response function of the cold atoms

A.1. Perturbing force on cold atoms subjected to a transient homogeneous magnetic field

The temporal profile of the bias field used in our experiments is shown in Fig. 7. We fit this profile with the following equation:

$$B_b(t)\begin{cases} = 0 & \text{if } t \le -w \\ = B_0\left(1 - e^{-\frac{t+w}{\tau_1}}\right) & \text{if } -w \le t \le 0 \\ = B_0\left(1 - e^{-\frac{w}{\tau_1}}\right) e^{-\frac{t}{\tau_2}} & \text{if} t \ge 0 \\ \simeq B_0\, e^{-\frac{t}{\tau_2}} & (\text{for } w >> \tau_1) \end{cases} \tag{22}$$

where, B_0 is the magnitude and w is the pulse width of the bias field, and where τ_1 and τ_2 are the rise time and fall time of the bias field. In our experiment, the values of τ_1 and τ_2 are 912 μs and 29.6 μs respectively. The approximation done in the last line of Eq. (22) is due to the fact that the time duration of the bias field (w = 5 sec) is much larger than the 912 μs rise time of the bias field. The exact values of τ_1 and τ_2 depend on the design details of the fast switching circuit for the magnetic field coils in Helmholtz configuration producing the bias field [29]. It is important to have a fast 'switching off' of the magnetic field so as to ensure that the measurements taken after switching off the magnetic field are not significantly affected by the time-constant τ_2. In any case, we incorporate the effect of τ_1 and τ_2 on the motion of the atoms in our theoretical model.

In a MOT, the x-component of the force on the cold atoms, which in [30] is expressed in terms of $x\,\partial B_m/\partial x$, can be recast as follows to show that the squared B-field acts like a potential energy for the atoms:

$$\begin{aligned} F_{MOT} &= -\alpha v - g\,\frac{\mu_B \lambda}{h}\,\alpha\, x\,\frac{\partial B_m}{\partial x} \\ &= -\alpha v - g\,\frac{\mu_B \lambda}{h}\,\alpha\,\frac{1}{2C_m}\,\frac{\partial B_m^2}{\partial x}. \end{aligned} \tag{23}$$

Here, $g = g_{F'} m_{F'} - g_F m_F$ for transition between the hyperfine levels $|F, m_F\rangle$ and $|F', m'_F\rangle$, μ_B is the Bohr magneton, λ is the wavelength of the cooling beams, h is the Planck's constant, and α

OPTICS CONTINUUM

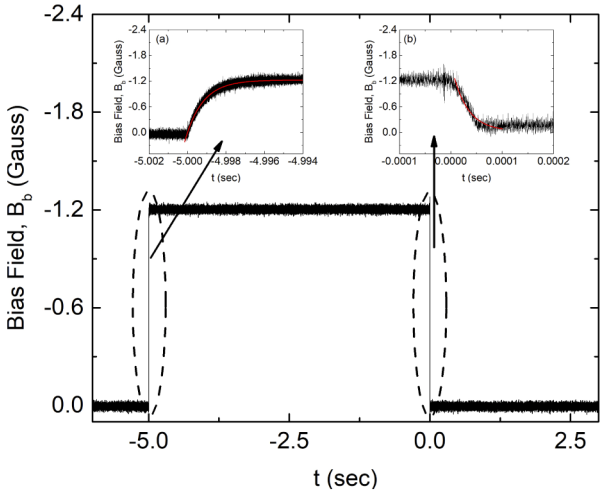

Fig. 7. Temporal profile of the bias field. The black solid line is the experimental data recorded using a closed-loop current transducer using Hall effect (LA 150 – P, from LEM USA Inc.) with a bandwidth of 150 kHz. Insets (a) and (b) show the growth and the decay, respectively, of the bias field as a function of time. After fitting the data using Eq. (22) we obtain $\tau_1 = (912 \pm 0.37)\,\mu s$ and $\tau_2 = (29.6 \pm 0.056)\,\mu s$.

is the damping coefficient. In the second line we have used that $B_m = C_m x$ with C_m a constant, which implies that

$$x\frac{\partial B_m}{\partial x} = \frac{B_m}{C_m}\frac{\partial B_m}{\partial x} = \frac{1}{2C_m}\frac{\partial B_m^2}{\partial x}.$$

In the presence of an additional bias field (B_b) along the negative x-direction, the force on an atom is given by (2) with the bias field added to B_m:

$$\begin{aligned} F_{net} &= -\alpha v - g\,\frac{\mu_B \lambda}{h}\,\alpha\,\frac{1}{2C_m}\,\frac{\partial (B_m - B_b)^2}{\partial x} \\ &= -\alpha v - g\,\frac{\mu_B \lambda}{h}\,\alpha\,\frac{1}{2C_m}\left(\frac{\partial B_m^2}{\partial x} - 2C_m B_b\right) \\ &= F_{MOT} + f(t) \end{aligned} \tag{24}$$

where we used that $\dfrac{\partial B_b}{\partial x} = 0$. Therefore

$$f(t) = g\,\frac{\mu_B \lambda}{h}\,\alpha\, B_b. \tag{25}$$

A.2. Mean displacement of the cold atoms

Using the expression for the position response function in Eq. (8) and the perturbing force in Eq. (25), we get

$$\langle x(t)\rangle = Ae^{\frac{(-\alpha+\alpha_c)\,t}{2M}} + Be^{\frac{-(\alpha+\alpha_c)\,t}{2M}} + Ce^{\frac{-t}{\tau_2}} \tag{26}$$

OPTICS CONTINUUM

where,

$$A = -\frac{2Mf_0}{\alpha_c}\left[\frac{\left(e^{\frac{(-\alpha+\alpha_c)w}{2M}}-1\right)}{\alpha-\alpha_c} - \frac{\tau_1\left(e^{\frac{(-\alpha+\alpha_c)w}{2M}} - e^{\frac{-w}{\tau_1}}\right)}{\alpha\tau_1 - 2M - \alpha_c\tau_1} + \frac{\tau_2\left(1-e^{\frac{-w}{\tau_1}}\right)}{\alpha\tau_2 - 2M - \alpha_c\tau_2}\right] \tag{27}$$

$$B = \frac{2Mf_0}{\alpha_c}\left[\frac{\left(e^{\frac{-(\alpha+\alpha_c)w}{2M}}-1\right)}{\alpha+\alpha_c} - \frac{\tau_1\left(e^{\frac{-(\alpha+\alpha_c)w}{2M}} - e^{\frac{-w}{\tau_1}}\right)}{\alpha\tau_1 - 2M + \alpha_c\tau_1} + \frac{\tau_2\left(1-e^{\frac{-w}{\tau_1}}\right)}{\alpha\tau_2 - 2M + \alpha_c\tau_2}\right] \tag{28}$$

$$C = \frac{4M\tau_2^2 f_0\left(1-e^{\frac{-w}{\tau_1}}\right)}{\left(4M^2 + \tau_2^2(\alpha^2-\alpha_c^2) - 4M\alpha\tau_2\right)}. \tag{29}$$

Here, $f_0 = g\,\frac{\mu_B\lambda}{h}\,\alpha\,B_0$ from Eq. (25).

The last term of Eq. (26) comes from the form of the perturbing force which was employed in our experiment. Its presence shows the advantage of using the fuller treatment over Eq. (18). Our results confirm the more complete model.

The mean velocity can also be obtained by taking a time derivative of $\langle x(t)\rangle$ in Eq. (26),

$$\langle v(t)\rangle = \frac{(\alpha_c-\alpha)A}{2M}e^{\frac{(-\alpha+\alpha_c)\,t}{2M}} - \frac{(\alpha+\alpha_c)B}{2M}e^{\frac{-(\alpha+\alpha_c)\,t}{2M}} - \frac{C}{\tau_2}e^{\frac{-t}{\tau_2}}. \tag{30}$$

Note that for negligible τ_1, τ_2 and for infinite width, i.e. $w \to \infty$, using Eq. (27), Eq. (28) and Eq. (29),

$$\frac{(\alpha_c-\alpha)A}{2M} \to -\frac{f_0}{\alpha_c}, \frac{(\alpha+\alpha_c)B}{2M} \to -\frac{f_0}{\alpha_c}, \frac{C}{\tau_2} \to 0$$

then, using Eq. (30) $\langle v(t)\rangle \to -f_0R(t)$ ($R(t)$ is given by Eq. (8)) and thus Eq. (16) is satisfied.

B. Spatial diffusion of cold atoms

We study the diffusive behaviour of the cold atoms in the viscous medium provided by our optical molasses, exploring different temperatures as the atomic cloud is cooled to lower temperatures via sub-Doppler cooling.

When the restoring force produced by the MOT magnetic field is absent, we are in the $k = 0$ regime of the Langevin equation which defines our theoretical model. We continue to assume that the dissipation kernel $\alpha(t)$ is simply a delta-function in time, or equivalently that the force exerted on an atom by the optical molasses is

$$F_{OM} = -\alpha v \tag{31}$$

where v is the velocity of the atom. For consistency, one would hope that essentially the same value of α would explain both the position response function studied above and the diffusive spreading studied here.

OPTICS CONTINUUM

As is well known, the mean-square distance traveled by the diffusing atom can be determined from the Langevin equation together with the noise-correlator, i.e. from Eqs. (1) and (3). The predicted time-dependence of the spreading depends on how the observation time τ compares with the "relaxation time" M/α. When $\tau \gg M/\alpha$ one finds the familiar Brownian motion, with diffusion coefficient D given by the Stokes-Einstein-Smoluchowski relation:

$$D = \frac{k_B T}{\alpha} \tag{32}$$

where k_B is the Boltzmann constant and T is the temperature of the cloud. However, for $\tau \ll M/\alpha$ one finds that the mean-square distance travelled grows like t^3 rather than t. In our experiment, the observation time of 20 ms is about 20 times bigger than $M/\alpha \sim 1$ ms. Although this is not enormously greater than unity, it seems sufficiently large to enable us to ignore the short-time crossover to t^3 spreading. We have therefore fitted the data under the assumption that we are in the regime of Brownian motion (Wiener process).

To observe the diffusive spreading of the atoms in the cold atomic cloud, we first loaded the MOT from the background Rb vapour. Thereafter, the MOT magnetic field was switched off, and the cloud was allowed to diffuse in the presence of the cooling laser beams forming the optical molasses, but still in the absence of the MOT magnetic field.

In the Brownian motion approximation, an atomic cloud of initial size of $(\Delta r)^2\big|_{t=0}$ expands to a size of $(\Delta r)^2\big|_{t=\tau}$ in time τ according to the relation:

$$(\Delta r)^2\big|_{t=\tau} = (\Delta r)^2\big|_{t=0} + 4\,D\,\tau, \tag{33}$$

where, Δr is the rms width of the cold atomic cloud.

We obtained $(\Delta r)^2$ directly from the column density profile of the absorption image at time t. In other similar experiments [31], the density profile was fitted to a Gaussian distribution, whereas the $(\Delta r)^2$ shown in Fig. 8 was obtained directly from the absorption images without assuming Gaussianity. This additional generality could become important in the quantum regime of logarithmic spreading, for which the analysis of [10] furnishes $(\Delta r)^2$ but not the full probability distribution of Δr. (We know of no proof that the latter will be Gaussian when the diffusion is not classical.)

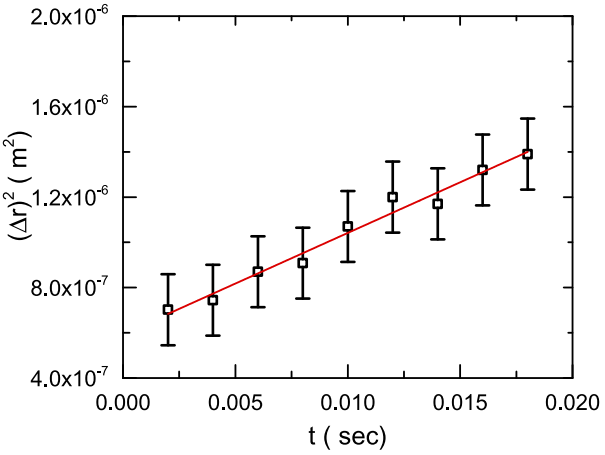

Fig. 8. The plot shows the atomic cloud size expanding in an optical molasses at a temperature of around $120\mu K$. The solid line is a fit to the experimental data using Eq. (33) .

Eq. (32) relates the damping coefficient α to the diffusion coefficient D and thereby allows us to check for consistency between our direct measurement of D (Fig. 8) and the value of the α

OPTICS CONTINUUM

deduced from our earlier measurements of the position response function. For a temperature of around $120\mu K$ of the cold atomic cloud, the diffusion coefficient obtained from the measurement of the diffusive spreading of the atomic cloud was $(1.01 \pm 0.15) \times 10^{-5}$ m^2/s yielding a value of $(1.58 \pm 0.25) \times 10^{-22}$ kg/s for α. For the same temperature, the value of α obtained from the measurement of the position response function was $(1.57 \pm 0.46) \times 10^{-22}$ kg/s. The agreement could not be better.

Funding. Ministry of Training, Colleges and Universities; Innovation, Science and Economic Development Canada; Ministry of Electronics and Information technology (4(7)/2020-ITEA); Department of Science and Technology, Ministry of Science and Technology, India (SR/WOS-A/PM-59/2019).

Acknowledgements. This work was partially supported by the Ministry of Electronics and Information Technology (MeitY), Government of India, through the Center for Excellence in Quantum Technology, under Grant4(7)/2020-ITEA. S.R acknowledges funding from the Department of Science and Technology, India, via the WOS-A project grant no. SR/WOS-A/PM-59/2019. This research was supported in part by Perimeter Institute for Theoretical Physics. Research at Perimeter Institute is supported in part by the Government of Canada through the Department of Innovation, Science and Economic Development Canada and by the Province of Ontario through the Ministry of Colleges and Universities. We acknowledge Hema Ramachandran, Meena M. S., Priyanka G. L. and RRI mechanical workshop for the instruments and assistance with the experiments.

Disclosures. The authors declare no conflicts of interest.

Data availability. Data underlying the results presented in this paper are not publicly available at this time but may be obtained from the authors upon reasonable request.

References

1. R. Kubo, "The fluctuation-dissipation theorem," Rep. Prog. Phys. **29**(1), 255–284 (1966).
2. G. F. Mazenko, *Nonequilibrium Statistical Mechanics* (Wiley, 2006).
3. R. Balescu, *Equilibrium and Non-Equilibrium Statistical Mechanics*, A Wiley interscience publication (Wiley, 1975).
4. A. Kumar, M. Rodriguez-Vega, T. Pereg-Barnea, and B. Seradjeh, "Linear response theory and optical conductivity of Floquet topological insulators," Phys. Rev. B **101**(17), 174314 (2020).
5. L. Pan, X. Chen, Y. Chen, and H. Zhai, "Non-Hermitian linear response theory," Nat. Phys. **16**(7), 767–771 (2020).
6. E. Barkai, E. Aghion, and D. A. Kessler, "From the Area under the Bessel Excursion to Anomalous Diffusion of Cold Atoms," Phys. Rev. X **4**(2), 021036 (2014).
7. L. Beilin, E. Gurevich, and B. Shapiro, "Diffusion of cold-atomic gases in the presence of an optical speckle potential," Phys. Rev. A **81**(3), 033612 (2010).
8. Y. Sagi, M. Brook, I. Almog, and N. Davidson, "Observation of Anomalous Diffusion and Fractional Self-Similarity in One Dimension," Phys. Rev. Lett. **108**(9), 093002 (2012).
9. S. Sinha and R. D. Sorkin, "Brownian motion at absolute zero," Phys. Rev. B **45**(14), 8123–8126 (1992).
10. U. Satpathi, S. Sinha, and R. D. Sorkin, "A quantum diffusion law," J. Stat. Mech.: Theory Exp. **2017**(12), 123105 (2017).
11. K. Kim, K.-H. Lee, M. Heo, H.-R. Noh, and W. Jhe, "Measurement of the trap properties of a magneto-optical trap by a transient oscillation method," Phys. Rev. A **71**(5), 053406 (2005).
12. G. W. Ford, J. T. Lewis, and R. F. O'Connell, "Quantum Langevin equation," Phys. Rev. A **37**(11), 4419–4428 (1988).
13. M. Hohmann, F. Kindermann, T. Lausch, D. Mayer, F. Schmidt, E. Lutz, and A. Widera, "Individual Tracer Atoms in an Ultracold Dilute Gas," Phys. Rev. Lett. **118**(26), 263401 (2017).
14. G. Volpe and G. Volpe, "Simulation of a Brownian particle in an optical trap," Am. J. Phys. **81**(3), 224–230 (2013).
15. Y. Deng, J. Bechhoefer, and N. R. Forde, "Brownian motion in a modulated optical trap," J. Opt. A: Pure Appl. Opt. **9**(8), S256–S263 (2007).
16. D. A. Kessler and E. Barkai, "Theory of Fractional Lévy Kinetics for Cold Atoms Diffusing in Optical Lattices," Phys. Rev. Lett. **108**(23), 230602 (2012).
17. R. Graham, "Langevin Equation of Collective Modes of Bose–Einstein Condensates in Traps," J. Stat. Phys. **101**(1/2), 243–257 (2000).
18. S. N. Majumdar and H. Orland, "Effective Langevin equations for constrained stochastic processes," J. Stat. Mech.: Theory Exp. **2015**(6), P06039 (2015).
19. A. Vulpiani and M. Baldovin, "Effective equations in complex systems: from Langevin to machine learning," J. Stat. Mech.: Theory Exp. **2020**(1), 014003 (2020).
20. In this paper, we have used the Langevin equation as the starting point, unlike [9, 10] where the FDT was used. Note, however, that the crucial input to the Langevin equation is the noise-noise correlation function given in Eq. (2), and this rests entirely on the FDT.
21. P. D. Lett, W. D. Phillips, S. L. Rolston, C. E. Tanner, R. N. Watts, and C. I. Westbrook, "Optical molasses," J. Opt. Soc. Am. B **6**(11), 2084 (1989).
22. R. Chang, A. L. Hoendervanger, Q. Bouton, Y. Fang, T. Klafka, K. Audo, A. Aspect, C. I. Westbrook, and D. Clément, "Three-dimensional laser cooling at the Doppler limit," Phys. Rev. A **90**(6), 063407 (2014).

OPTICS CONTINUUM

23. In the experimental setup, the spring constant k of the MOT is always finite. Therefore one cannot achieve the k=0 limit of the position response function in Eq. (8) which corresponds to the position response function used in [10]. Nevertheless, we get a very good agreement between our theory and experimental data for all finite values of k.
24. M. Fan, C. A. Holliman, A. L. Wang, and A. M. Jayich, "Laser Cooling of Radium Ions," Phys. Rev. Lett. **122**(22), 223001 (2019).
25. J. F. Sherson, C. Weitenberg, M. Endres, M. Cheneau, I. Bloch, and S. Kuhr, "Single-atom-resolved fluorescence imaging of an atomic Mott insulator," Nature **467**(7311), 68–72 (2010).
26. W. S. Bakr, J. I. Gillen, A. Peng, S. Fölling, and M. Greiner, "A quantum gas microscope for detecting single atoms in a Hubbard-regime optical lattice," Nature **462**(7269), 74–77 (2009).
27. L. Amico, G. Birkl, M. Boshier, and L.-C. Kwek, "Focus on atomtronics-enabled quantum technologies," New J. Phys. **19**(2), 020201 (2017).
28. A. Das, A. Dhar, I. Santra, U. Satpathi, and S. Sinha, "Quantum Brownian motion: Drude and Ohmic baths as continuum limits of the Rubin model," Phys. Rev. E **102**(6), 062130 (2020).
29. C. J. Dedman, K. G. H. Baldwin, and M. Colla, "Fast switching of magnetic fields in a magneto-optic trap," Rev. Sci. Instrum. **72**(11), 4055–4058 (2001).
30. C. J. Foot, *Atomic Physics*, Oxford Master Series in Atomic, Optical and Laser Physics (Oxford University Press, Oxford, 2007).
31. T. W. Hodapp, C. Gerz, C. Furtlehner, C. I. Westbrook, W. D. Phillips, and J. Dalibard, "Three-dimensional spatial diffusion in optical molasses," Appl. Phys. B **60**(2-3), 135–143 (1995).